



A novel technique to quantify glioma tumor invasion using serial microscopy sections

N. Shastry Akella^{a,1}, Qiang Ding^{b,1}, Ingrid Menegazzo^{b,c},
Wenquan Wang^d, G. Yancey Gillespie^e, J. Robert Grammer^b,
Candece L. Gladson^{b,*,2}, L. Burton Nabors^{a,2,3}

^a Department of Neurology, Division of Neuro-Oncology, University of Alabama at Birmingham, Birmingham, AL 35294, USA

^b Department of Pathology, Division of Neuropathology, University of Alabama at Birmingham, Birmingham, AL 35294, USA

^c Department of Biomedical Engineering, University of Alabama at Birmingham, Birmingham, AL 35294, USA

^d Department of Medicine, Division of Hematology Oncology, Biostatistics Section,
University of Alabama at Birmingham, Birmingham, AL 35294, USA

^e Department of Surgery, Division of Neurosurgery, University of Alabama at Birmingham, Birmingham, AL 35294, USA

Received 8 July 2005; received in revised form 24 October 2005; accepted 28 October 2005

Abstract

Here we present a new technique to quantitatively characterize malignant glioma invasion in a syngeneic mouse model. The GL261 mouse malignant glioma cell line was injected intracerebrally into the C57B1/6 black mouse and allowed to propagate for 10 or 17 days, followed by euthanasia of the animal, harvesting of the brain, fixation, and serial sectioning. Histologic examination was performed and the primary tumor mass and discontinuous sites of tumor invasion were traced on digital images of serial microscopy sections, followed by analysis of the invasion characteristics using a custom-written MATLAB program. We found a significant increase in the number of discontinuous tumor invasion sites and in the distance of these sites from the tumor centroid in mice that were euthanized at 17 days post-tumor cell injection, as compared to mice euthanized at 10 days. Furthermore, a scatter plot analyses indicated that the invasion site data could be grouped based on the characteristics of area and distance from the tumor centroid to reveal significant differences between the two experimental groups of mice. This quantitative method will allow a future in vivo analysis of invasion characteristics in glioma cells expressing altered levels or function of invasion genes, and of new therapy targeting invading glioma cells.

© 2005 Elsevier B.V. All rights reserved.

Keywords: Glioma; Invasion; Glioblastoma; Mathematical models; Serial microscopy; Animal models

1. Introduction

The mechanisms regulating the invasive phenotype of malignant glioma tumors are not well understood. This is of tremendous clinical importance, as local and distant tumor invasion are likely responsible, in large part, for the considerable morbidity and mortality of malignant glioma tumors (Bolteus et al., 2001; Giese et al., 2003). Tumor growth and invasion occur in a complex microenvironment that is regulated by both tumor

cells and host stromal cells (Tysnes and Mahesparan, 2001; Thorsen and Tysnes, 1997). Clinical and experimental data have shown that glioma invasion is dependent on multiple mechanisms that include protease digestion of the extracellular matrix, tumor cell migration promoted by the cooperation of integrin and growth factor receptors, the activation of signaling effectors downstream of integrin and growth factor receptors that promote membrane protrusion and ultimately cell migration, as well as cell attachment to the extracellular matrix at a new site (Giese et al., 2003; Rao, 2003; Gladson et al., 1995a,b; Ding et al., 2002, 2003). Angiogenesis, the development of new microvessels, also promotes tumor invasion and is a prominent histologic feature of malignant glioma tumors (Bolteus et al., 2001; Thorsen and Tysnes, 1997). The mechanisms regulating angiogenesis are complex, but they include cytokine-mediated transcriptional regulation of pro-angiogenic factors, and the

* Corresponding author. Tel.: +1 205 975 7847; fax: +1 205 934 7346.

E-mail addresses: gladson@uab.edu (C.L. Gladson), bnabors@uab.edu (L.B. Nabors).

¹ Both the authors contributed equally and share the first authorship.

² Co-senior authors.

³ Tel.: +1 205 934 1813; fax: +1 205 975 7546.

expression of endogenous inhibitors of angiogenesis by host stromal cells (Nabors et al., 2001, 2003; Rege et al., 2005). Surgical resection of malignant gliomas is part of the current clinical treatment; however, sites of tumor invasion are frequently not visually detectable, and thus these sites of tumor are left in the brain to proliferate.

To date, the semi-quantitative techniques used to evaluate glioma tumor invasion in tissue sections have relied on a combination of traditional staining, vital dyes, and fluorescent laser microscopy. Matsumura et al. (2000) demonstrated malignant glioma cell invasion into a brain slice maintained in organotypic culture, and also found elevated levels of matrix metalloprotease (MMP)-2 and -9 at the invading glioma cells. De Bouard et al. (2002) cultured glioma biopsy specimens on slices of rodent brain, and found preferential invasion of the glioma cells along blood vessels in the normal brain slices. The distance of tumor cell migration/invasion was 2–4-fold greater when malignant glioma biopsy specimens were cultured on the brain slices, as compared to the similar culture of low-grade glioma biopsy specimens. These reports suggest that high-grade gliomas are more invasive and that there is likely a role for MMPs in promoting glioma invasion.

Whether tumor cell invasion and proliferation are independent or linked events in the life of tumor cells is not entirely clear. Schiffer et al. (1997) evaluated the mitotic and proliferating cell nuclear antigen (PCNA) labeling indices of groups of invading cells in autopsy brain sections from 90 patients with glioblastoma (malignant glioma) tumors. They found that when the interface between the solid tumor and the adjacent brain was represented by a gradient of tumor cell density, the proliferation labeling index was either unchanged or it was lower in the interface. When the interface between the solid tumor and the adjacent brain was represented by a clear demarcation of tumor, there was a high density of labeled nuclei at the tumor periphery. Giese et al. (1996) utilizing in vitro invasion assays have reported that the invading glioma cells are not proliferating. Thus, the relationship between invasion and proliferation in malignant gliomas is likely complex. An understanding of the molecular steps involved in tumor cell invasion in vivo is dependent on the availability of quantitative tools for characterizing tumor invasion. To the best of our knowledge, there is currently no commercially available software to compute quantitative tumor invasion site characteristics in a three-dimensional model with respect to a reference point. In this report, we demonstrate the application of such a technique that is applied to a syngeneic intracerebral mouse model of invasive malignant glioma. The availability of such an image processing technique will significantly augment the ability to analyze stained serial microscopy sections of glioma tumors.

2. Materials and methods

2.1. Cells

The GL261 mouse malignant glioma cells were obtained from the NCI-Frederick Cancer Research National Tumor

Repository, and were propagated in DMEM media with 10% fetal bovine serum.

2.2. Animal model and histology

GL261 cells were harvested with buffered EDTA, washed, re-suspended in PBS, and 100,000 cells in 5 μ l of PBS injected with stereotactic assistance into the basal ganglia of the C57B1/6 black mouse brain, as described previously (Wang et al., 2000). The tumors were allowed to propagate for 10 or 17 days, at which point the animals were euthanized, the brains harvested and fixed in buffered formalin, followed by embedding in paraffin. All animal studies were performed in accordance with the Animal Welfare Act (PL99-158), and the *Guide of the Care and Use of Laboratory Animals*.

The brains were serially sectioned (7 μ m sections), and a section every 70 μ m stained with hematoxylin and eosin. Five sections from each mouse brain were used for the analyses described in this report. Histologic analyses of serial microscopy sections were performed using a Leica DMR microscope (Leica Microsystems AG, Wetzlar, Germany). The main tumor mass as well as the sites of discontinuous tumor invasion were traced on digital images by a neuropathologist (CLG), and imported into custom-written image processing programs for further processing. A discontinuous invasion site was defined as a site of multiple (≥ 3) tumor cells that were not directly connected to the main tumor mass.

2.3. Quantification of tumor invasion

The processing tools for tumor invasion site computations were custom-written in MATLAB (MathWorks Inc., Natick, MA). The mouse brain sections for each animal were co-registered and stacked for three-dimensional invasion computation. Anatomic reference points were selected for geometric correction based on the position of the cingulum, stria terminalis, cortex cerebri, and the ventricles. The serial sections were rotated and translated with reference to a central section that contained the injection site. For the data presented in this report, all images were acquired at the same magnification (1.6 \times) and thus scaling was not performed, although it has been incorporated into our image-processing program as an optional function for more complex microscopy.

A tumor centroid was computed for each mouse by calculating the planar center of mass of the main tumor mass in the central section (site of tumor cell injection). An estimate of the tumor volume was computed by summing the area of the main tumor mass calculated in pixels from each of the five sections, as described previously (Wang et al., 2000; Ding et al., 2005). A procedural flowchart for the steps described above is shown in Fig. 1.

2.4. Statistical analyses

For each animal, the number of discontinuous invasion sites, the three-dimensional distance from the tumor centroid in μ m,

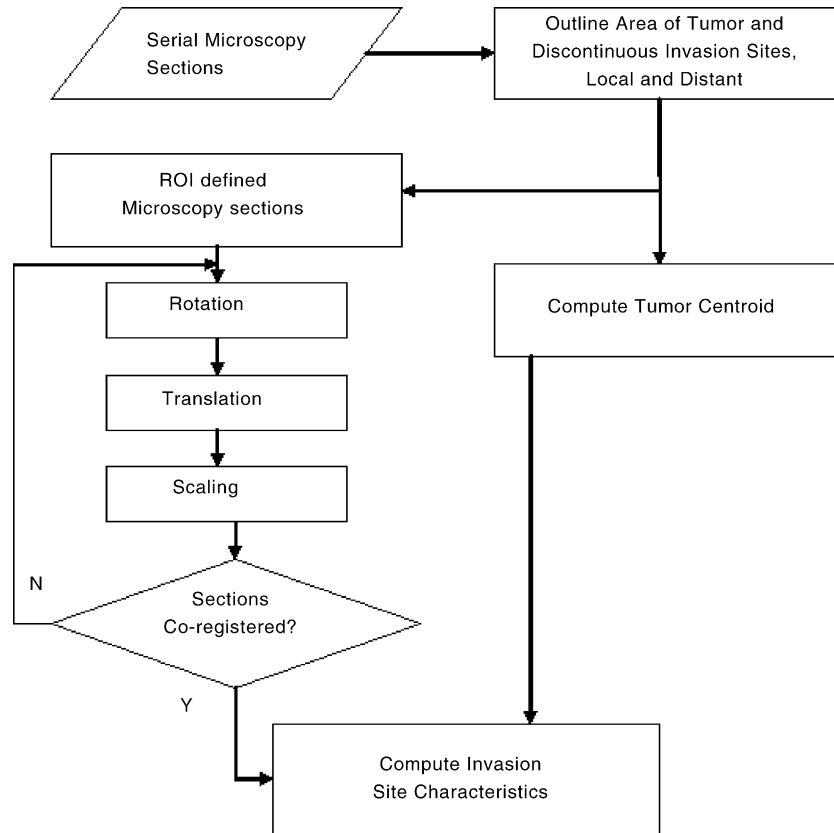


Fig. 1. Flowchart of the steps in computing tumor invasion site characteristics.

the area of each invasion site in μm^2 , and the estimated tumor volume in mm^3 were calculated along with the corresponding mean, standard deviation, median, and range. Due to the small number of mice, a one-sided Wilcoxon's rank sum test using normal approximation was applied to compare the number of discontinuous invasion sites, and the percentage of invasion sites falling into four groups that were statistically determined to be different using mean areas and invasion site distances for all eight animals. The estimated main tumor volume for all mice, as well as the invasion area and distance for the 10 sites of discontinuous invasion with the largest area for each mouse were also compared between animals euthanized at 10 and 17 days. The significance level was set at 0.05. All statistical analyses were performed using the SAS software (version 9.00, SAS Institute Inc., Cary, NC).

3. Results

3.1. Quantitation of tumor invasion sites

An example of an image series corrected and stacked using our program is shown in Fig. 2. The number of discontinuous invasion sites, the distance of each discontinuous invasion site from the tumor centroid, and the area of each discontinuous invasion site calculated for each animal brain are presented in Table 1.

3.2. Grouping of data

The mean distance of invasion from the tumor centroid for each mouse and the mean area of invasion for all sites of discontinuous tumor invasion for each mouse were calculated from all eight mice, and were $2732 \mu\text{m}$ and $11,808 \mu\text{m}^2$, respectively. Based on these numbers we then categorized the invasion sites in each mouse brain into four groups (Table 2 and Figs. 3 and 4) as

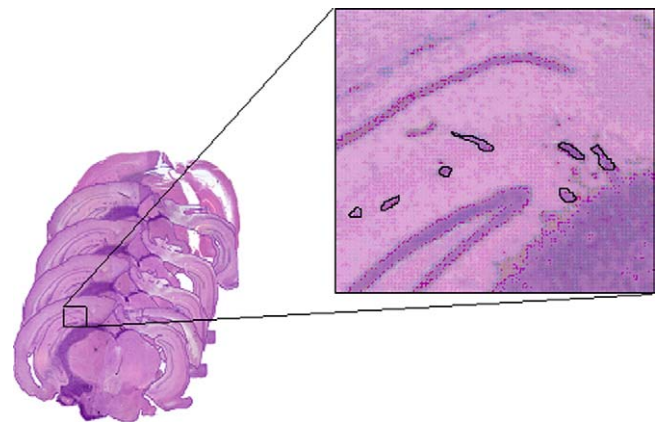


Fig. 2. Hematoxylin and eosin-stained microscopy sections, corrected, and readied for invasion site analyses using our technique. The inset shows tumor invasion sites outlined for quantitative characterization.

Table 1
Tumor invasion sites: distance and area

Mouse	Day of euthanasia	Number of invasion sites	Distance from tumor centroid (μm)				Area of invasion sites (μm^2)			
			Mean	S.D. ^a	Median	Range	Mean	S.D.	Median	Range
1	10	138	2295	831	2432	332–4261	9556	5483	8613	525–33325
2	10	129	2337	689	2231	915–4682	8440	5749	6925	925–29600
3	10	131	2536	1590	2007	181–6406	9839	11727	6200	1225–68250
4	10	350	2242	945	2144	273–4441	10898	7999	8875	925–65500
5	17	212	2623	782	2688	944–4594	11678	10498	8938	550–96825
6	17	597	2832	1580	2536	168–7415	11558	14386	8925	900–232930
7	17	397	3552	1970	2960	349–8675	9807	9563	7475	925–96275
8	17	630	2648	1266	2591	99–5999	15446	18206	9963	575–192780

^a Standard deviation.

Table 2
Summary of invasion site grouping (% of invasion sites in each group)

Mouse	Day of euthanasia	Number of invasion sites	Group 1 (distance < 2732; area < 11808)	Group 2 (distance < 2732; area \geq 11808)	Group 3 (distance \geq 2732; area < 11808)	Group 4 (distance \geq 2732; area \geq 11808)
1	10	138	55.8	16.7	18.8	8.7
2	10	129	53.5	20.9	24.8	0.8
3	10	131	57.3	13.0	22.9	6.9
4	10	350	47.1	20.6	21.4	10.9
5	17	212	35.4	17.5	29.7	17.5
6	17	597	35.9	18.1	32.3	13.7
7	17	397	30.0	12.3	44.3	13.4
8	17	630	29.4	24.6	27.6	18.4

follows: Group (1), the mean distance from the tumor centroid <2732 μm and the mean area of invasion sites <11,808 μm^2 ; Group (2), the mean distance from the tumor centroid <2732 μm and the mean area of invasion sites \geq 11,808 μm^2 ; Group (3), the

mean distance from the tumor centroid \geq 2732 μm and the mean area of invasion sites <11,808 μm^2 ; and Group (4), the mean distance from the tumor centroid \geq 2732 μm and the mean area of invasion sites \geq 11,808 μm^2 .

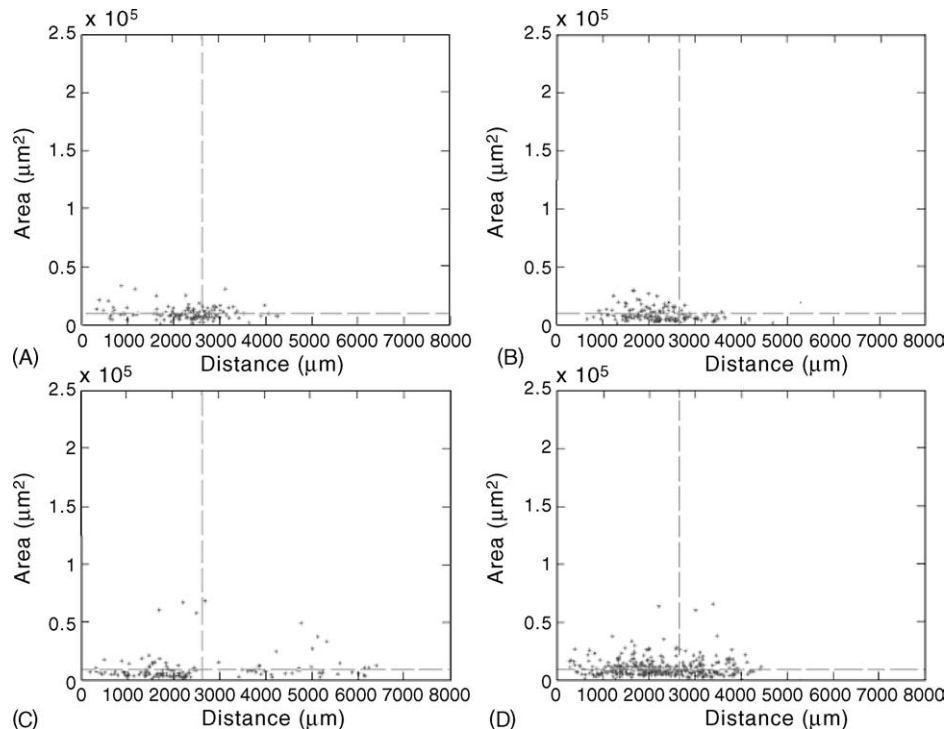


Fig. 3. Scatter plots showing the invasion site distance vs. area for brains from mice euthanized at 10 days: (A) mouse 1, (B) mouse 2, (C) mouse 3 and (D) mouse 4.

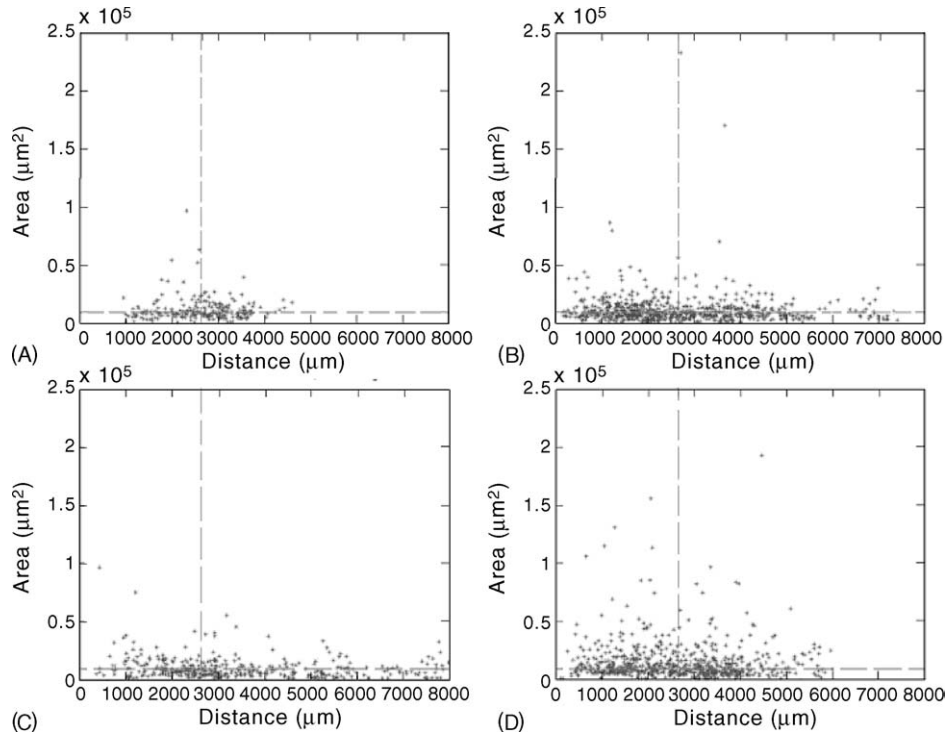


Fig. 4. Scatter plots showing the invasion site distance vs. area for brains from mice euthanized at 17 days: (A) mouse 5, (B) mouse 6, (C) mouse 7 and (D) mouse 8.

3.3. Longitudinal comparison between groups

A one-sided Wilcoxon's rank sum test using normal approximation was then applied to compare the number and the percentage of discontinuous invasion sites falling into Group (4) for mice euthanized at 10 days versus 17 days. This statistical analysis was also applied to compare the mean distance from the tumor centroid and the mean area of the discontinuous invasion sites using the means of each mouse between the two groups of mice euthanized at 10 or 17 days. In the mice euthanized at 17 days, we found a greater total number of discontinuous invasion sites ($p=0.0303$), a greater number of discontinuous invasion sites that fell into Group (4) ($p=0.0152$), and a greater mean distance of the discontinuous invasion sites from the tumor centroid ($p=0.0152$), as compared to the mice euthanized at 10 days (Figs. 3 and 4; Table 3). In the mice euthanized at 17 days, we also found that the mean area of discontinuous invasion sites was larger as compared to the mice euthanized at 10 days, and this difference was marginally significant ($p=0.0562$) (Table 3).

In the group of mice euthanized at 10 days, the estimated mean tumor volume was 2.49 mm^3 , with a standard deviation

of 0.41 mm^3 , and a median of 2.52 mm^3 . In the group of mice euthanized at 17 days, the estimated mean tumor volume was 7.68 mm^3 with a standard deviation of 3.57 mm^3 and a median of 6.99 mm^3 . Based on the Wilcoxon rank sum test, a one-sided p value of 0.0152 was found when comparing the difference between the two experimental groups of mice. The main tumor volume of the animals studied is illustrated in Fig. 5. The largest tumor, in mouse 6, was 12.627 mm^3 , which is the size of a cube with sides of approximately 2.329 mm.

In comparing the 10 sites of discontinuous invasion with the largest area for each mouse, we found a significant increase in the mean area of the discontinuous invasion sites, and in the mean distance of the discontinuous invasion sites from the tumor centroid in the mice euthanized at 17 days ($p=0.0152$ and 0.0970 ,

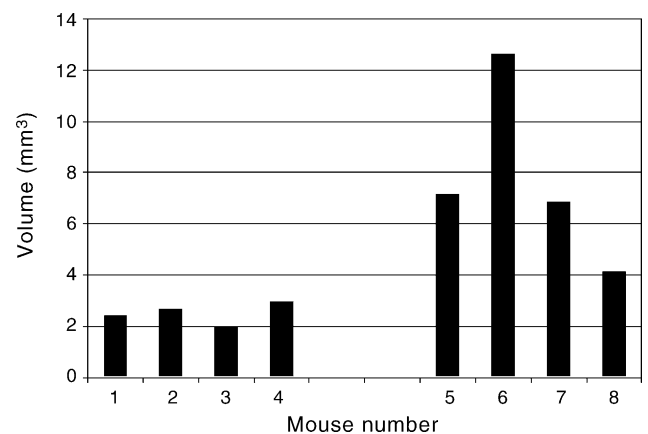


Fig. 5. Estimated main tumor volume. Mice 1–4 were euthanized at 10 days, and mice 5–8 at 17 days.

Table 3
Comparisons between the two experimental groups of mice

	Mice euthanized at 10 days	Mice euthanized at 17 days	p^a
Number of invasion sites	187	459	0.0303
Mean distance	2353	2914	0.0152
Mean area	9683	12122	0.0562
% of Group (4)	6.83	15.75	0.0152

^a Determined using a one-sided Wilcoxon rank sum test.

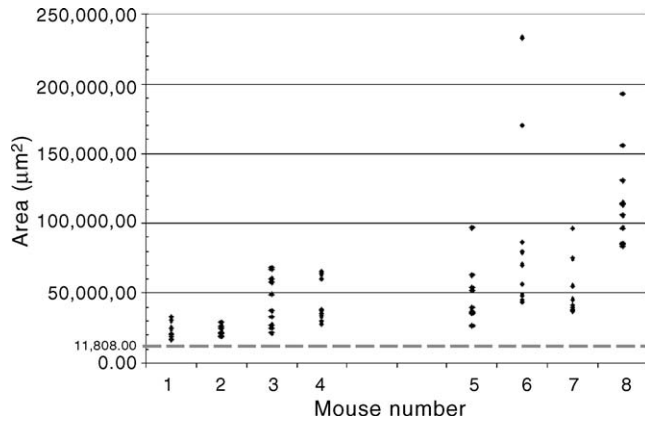


Fig. 6. Scatter plot of the 10 largest invasion sites in the mice.

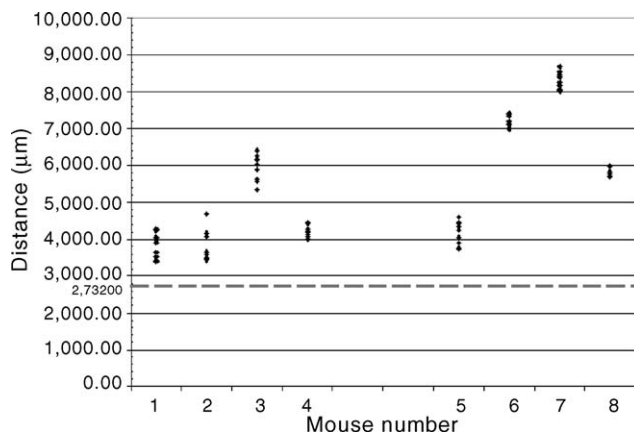


Fig. 7. Scatter plot of the 10 invasion site foci in each mouse with the greatest distance from the tumor centroid.

respectively), as compared to the mice euthanized at 10 days (Figs. 6 and 7 and Tables 4 and 5). These data collectively suggest that the tumors in the mice euthanized at 17 days demonstrate a greater evidence of discontinuous tumor invasion, as compared to the tumors in the mice euthanized at 10 days.

Table 4
Summary of the GL261 histologic analysis for the 10 largest invasion sites in animals euthanized at 10 days

Mouse	Main tumor volume pixels (mm ³)	Mean area (µm ²)	Maximum area (µm ²)	Mean distance (µm)	Maximum distance (µm)
1	2.404	23730.00	33325.00	3829.91	4261.80
2	2.640	23377.50	29600.00	3770.94	4932.50
3	1.976	44685.00	68250.00	5950.26	6405.70
4	2.954	41952.50	65500.00	4189.26	4441.20

Table 5
Summary of the GL261 histologic analysis for the 10 largest invasion sites in animals euthanized at 17 days

Mouse	Main tumor volume pixels (mm ³)	Mean area (µm ²)	Maximum area (µm ²)	Mean distance (µm)	Maximum distance (µm)
5	7.124	46742.50	96825.00	4153.14	4593.80
6	12.627	87771.00	232930.00	7152.88	7414.50
7	6.854	50397.50	96275.00	8275.73	8674.80
8	4.101	116442.00	192780.00	5784.53	5999.00

4. Discussion

The development of quantitative techniques for the evaluation of tumor invasion is of particular importance for malignant glioma tumors, as the invasive phenotype of this tumor contributes significantly to the morbidity and mortality of the disease. Elucidation of the molecular alterations that promote the invasive phenotype in animal models requires the development of specialized quantitative methods. We report here the development of a quantitative technique to evaluate tumor cell invasion in serial microscopy sections of glioma-bearing mouse brains by computing three-dimensional discontinuous invasion site characteristics with respect to a reference point. The characteristics of invading glioma cells that were quantified here include the number of discontinuous invasion sites, the area of the individual invasion sites, and the distance of the invasion sites from the tumor centroid. We found the mean number of discontinuous invasion sites and the mean distance of these invasion sites from the tumor centroid to be significantly larger in the tumor-bearing brains from animals euthanized at 17 days, as compared to the animals euthanized at 10 days. As one would expect, an increased evidence of invasion over time in an invasive model of malignant glioma, these data support the validity of our new approach quantitating invasion site characteristics. The invasive histologic features of this animal model of malignant glioma were described by Zagzag et al. (2000), and are highly similar to the human disease; thus, this is an ideal animal model in which to validate our new approach and custom-written computer program.

Although the temporal quantification of the number of invasion sites and of the distance of the invasion sites from the tumor centroid were significantly different when comparing tumors propagated intracerebrally for 10 or 17 days, a potential weakness of our approach is that it requires identification of tumor cells by a neuropathologist. For some research groups this could limit the usefulness of the approach. Also, there is a resolution limit when identifying tumor cells by histologic examination. This can be overcome by utilizing glioma cell lines with unique markers, such as the expression of cell surface proteins that

could be recognized by immunohistochemistry, or green fluorescent protein (GFP) that would be amendable to fluorescent microscopy or immunostain. For example, Zagzag et al. (2003) reported the propagation of the GFP-transfected GL261 cells in the C57B1/6 mouse brain. We did not use GL261 cells stably expressing GFP for this study, as we found that GFP–GL261 cells expressing high levels of GFP proliferated at a slower rate in the mouse brain as compared to the wild-type GL261 cells (J.R. Grammer and C.L. Gladson, unpublished observation).

In summary, we report a quantitative method to evaluate glioma tumor cell invasion in the in vivo brain environment. Our analysis of invasion site characteristics which include calculating the area of discontinuous invasion sites and the distance from a reference point (the tumor centroid) could yield valuable information regarding disease progression over time. The quantitation of such parameters could also aid in the comparative evaluation of invasion in other models of glioma, as this technique is easily extended to other models where histopathology is obtained. The ability to quantify the invasive phenotype is critical to future animal studies investigating the molecular events promoting glioma cell invasion and to pre-clinical animal studies testing agents that potentially inhibit glioma invasion.

Acknowledgements

This work was supported by the following grants from the National Institutes of Health, National Cancer Institute: CA097247 (G.Y.G., C.L.G., L.B.N.); CA97110 (C.L.G.); CA091560 (L.B.N.); and a National Brain Tumor Foundation grant (Q.D.). The authors would also like to thank Mrs. Jo Self for assistance in the preparation of this manuscript.

References

- Bolteus AJ, Berens ME, Pilkington GJ. Migration and invasion in brain neoplasms. *Curr Neurol Neurosci Rep* 2001;1:225–32.
- De Bouard S, Christov C, Guillamo JS, Kassas-Duchossoy L, Palfi S, Leguerinel C, et al. Invasion of human glioma biopsy specimens in cultures of rodent brain slices: a quantitative analysis. *J Neurosurg* 2002;97:169–76.
- Ding Q, Stewart Jr J, Prince CW, Chang PL, Trikha M, Han X, et al. Promotion of malignant astrocytoma cell migration by osteopontin expressed in the normal brain: differences in integrin signaling during cell adhesion to osteopontin versus vitronectin. *Cancer Res* 2002;62:5336–43.
- Ding Q, Stewart Jr J, Olman MA, Klobe MR, Gladson CL. The pattern of enhancement of Src kinase activity on platelet-derived growth factor stimulation of glioblastoma cells is affected by the integrin engaged. *J Biol Chem* 2003;278:39882–91.
- Ding Q, Grammer JR, Nelson MA, Guan J-L, Stewart Jr JE, Gladson CL. p27^(Kip1) and cyclin D1 are necessary for focal adhesion kinase (FAK) regulation of cell cycle progression in glioblastoma cells propagated in vitro and in vivo in the scid mouse brain. *J Biol Chem* 2005;280:6802–15.
- Giese A, Loo MA, Tran N, Haskett D, Coons SW, Berens ME. Dichotomy of astrocytoma migration and proliferation. *Int J Cancer* 1996;67:275–82.
- Giese A, Bjerkvig R, Berens ME, Westphal M. Cost of migration: invasion of malignant gliomas and implications for treatment. *J Clin Oncol* 2003;21(8):1624–36.
- Gladson CL, Pijuan-Thompson V, Olman MA, Gillespie GY, Yacoub IZ. Up-regulation of urokinase and urokinase receptor genes in malignant astrocytoma. *Am J Pathol* 1995a;146:1150–60.
- Gladson CL, Wilcox JN, Gillespie GY, Sanders L, Cheresch DA. Cerebral microenvironment influences expression of the vitronectin gene in astrocytic tumors. *J Cell Sci* 1995b;108:947–56.
- Matsumura H, Ohnishi T, Kanemura Y, Maruno M, Yoshimine T. Quantitative analysis of glioma cell invasion by confocal laser scanning microscopy in a novel brain slice model. *Biochem Biophys Res Commun* 2000;269:513–20.
- Nabors LB, Gillespie GY, Harkins L, King PH. HuR, a RNA stability factor, is expressed in malignant brain tumors and binds to adenine-and uridine-rich elements within the 3' untranslated regions of cytokine and angiogenic factor mRNAs. *Cancer Res* 2001;61:2154–61.
- Nabors LB, Suswam E, Huang Y, Yang X, Johnson MJ, King PH. Tumor necrosis factor α induces angiogenic factor up-regulation in malignant glioma cells: a role for RNA stabilization and HuR. *Cancer Res* 2003;63:4181–7.
- Rao JS. Molecular mechanisms of glioma invasiveness: the role of proteases. *Nat Rev Cancer* 2003;3:489–501.
- Rege TA, Fears CY, Gladson CL. Endogenous inhibitors of angiogenesis in malignant gliomas: nature's angiogenic therapy. *Neuro-Oncology* 2005;7:106–21.
- Schiffer D, Cavalla P, Dutto A, Borosotti L. Cell proliferation and invasion in malignant gliomas. *Anticancer Res* 1997;17:61–70.
- Thorsen F, Tysnes BB. Brain tumor cell invasion, anatomical and biological considerations. *Anticancer Res* 1997;17:4121–6.
- Tysnes BB, Mahesparan R. Biological mechanisms of glioma invasion and potential therapeutic targets. *Neuro-Oncology* 2001;53:129–47.
- Wang D, Grammer JR, Cobbs CS, Stewart Jr JE, Liu Z, Rhoden R, et al. p125 focal adhesion kinase promotes malignant astrocytoma cell proliferation in vivo. *J Cell Sci* 2000;113:4221–30.
- Zagzag D, Amirnovin R, Greco MA, Yee H, Holash J, Wiegand SJ, et al. *Lab Invest* 2000;80:837–49.
- Zagzag D, Miller DC, Chiriboga L, Yee H, Newcomb EW. Green fluorescent protein immunohistochemistry as a novel experimental tool for the detection of glioma cell invasion in vivo. *Brain Pathol* 2003;13(1):34–7.